Title

Hourly and daily rainfall intensification causes opposing effects on C and N emissions, storage, and leaching in dry and wet grasslands

Journal

Biogeochemistry, 144(2)

ISSN

0168-2563

Authors

Tang, Fiona HM
Riley, William J
Maggi, Federico

Publication Date

2019-07-01

DOI

10.1007/s10533-019-00580-7

Peer reviewed

Hourly and daily rainfall intensification causes opposing effects on C and N emissions, storage, and leaching in dry and wet grasslands

Fiona H. M. Tang . William J. Riley . Federico Maggi

F. H. M. Tang, F. Maggi: Laboratory for Advanced Environmental Engineering Research, School of Civil Engineering, The University of Sydney, Bld. J05, Sydney, NSW 2006, Australia e-mail: fiona.tang@sydney.edu.au; W. J. Riley: Earth Sciences Division, Lawrence Berkeley National Laboratory, Berkeley, CA 94720, USA

Abstract

Climate change is expected to alter hourly and daily rainfall regimes and, in turn, the dynamics of ecosystem processes controlling greenhouse gas emissions that affect climate. Here, we investigate the effects of expected twenty-first century changes in hourly and daily rainfall on soil carbon and nitrogen emissions, soil organic matter (SOM) stocks, and leaching using a coupled mechanistic carbon and nitrogen soil biogeochemical model (BAMS2). The model represents various abiotic and biotic processes involving 11 SOM pools. These processes include fungal depolymerization, heterotrophic bacterial mineralization, nitrification, denitrification, microbial mortality, necromass decomposition, microbial response to water stress, protection, aqueous advection and diffusion, aqueous complexation, and gaseous dissolution. Multi-decadal modeling with varying rainfall patterns was conducted on nine Australian grasslands in tropical, temperate, and semi-arid regions. Our results show that annual CO_2 emissions in the semi-arid grasslands increase by more than 20% with a 20% increase in annual rainfall (with no changes in the rainfall timing), but the tropical grasslands have opposite trends. A 20% increase in annual rainfall also increases annual N_2O and NO emissions in the semi-arid grasslands by more than 10% but decreases emissions by at least 25% in the temperate grasslands. When subjected to low frequency and high magnitude daily rainfall events with unchanged annual totals, the semi-arid grasslands are the most sensitive, but changes in annual CO_2 emissions and SOM stocks are less than 5%. Intensification of hourly rainfall did not significantly alter CO_2 emissions and SOM stocks but changed annual NH_3 emissions in the tropical grasslands by more than 300%.

Keywords: Soil organic carbon, Carbon cycle, Nitrogen cycle, SOM model, Precipitation

Introduction

Climate change is predicted to increase rainfall temporal variability, with a consensus of a shift towards a higher frequency of droughts and heavier rainfall events (Easterling et al. 2000; Zhang et al. 2013). Although the uncertainty in rainfall predictions is high and the predicted changes are spatially heterogeneous (Maslin and Austin 2012), trend-detection studies based on global and regional rainfall datasets have consistently reported an intensification in daily (Donat et al. 2013; Fischer and Knutti 2014) and hourly (Guerreiro et al. 2018) extremes. Changes in rainfall regimes can increase variations in soil water content, which is a key driver of ecosystem processes that affects vegetation growth (Porporato et al. 2003; Yu et al. 2017; Tietjen et al. 2017), soil respiration (Curiel Yuste et al. 2007; Schimel 2018), biogeochemical cycles (Delgado-Baquerizo et al. 2013; Nielsen and Ball 2015), and greenhouse gas emissions (e.g., CO_2, CH_4, NO_x; Harper et al. 2005; Kim et al. 2012). Hence, it is essential to analyze the extent to which rainfall variability can affect terrestrial carbon and nitrogen emissions.

Predicting the dynamics of soil organic matter (SOM) as a result of rainfall intensification is complex and has been the target of many research efforts. On the one hand, decreased rainfall amount can suppress SOM depolymerization and mineralization due to stronger microbial water stress (Schimel et al. 2007) and reduced nutrient mobility (Manzoni et al. 2012), leading to a reduction in CO_2 emissions. On the other hand, rainfall extremes can increase the frequency of drying-rewetting cycles that result in CO_2 pulses a few orders of magnitudes higher than background emissions (known as “the *Birch effect*”, Birch 1958; Li et al. 2010; Vargas et al. 2010). Studies based on single and multiple cycles of drying-rewetting experiments have arrived at very different conclusions regarding the carbon sources and mechanisms contributing to the observed CO_2 pulses (Schimel 2018). The proposed mechanisms include contributions from dead microbial biomass (Kieft 1987), mobilization of stable carbon (Navarro-García et al. 2012), microbial intracellular osmolytes (Warren 2014), and microbial resuscitation (Placella et al. 2012). Most of these experiments, however, were conducted at a time-scale of days to months and, hence it is difficult to extrapolate the observed drying-rewetting effects to long-term emissions and carbon storage. In addition to microbial mediated processes, heavy rainfall pulses can increase SOM losses through leaching in the form of dissolved organic (DOC) and inorganic carbon (DIC) (Liu et al. 2018). CO_2 efflux may be suppressed by reduced gas mobility in wet soil (Bouma and Bryla 2000); as a consequence, DIC is more prone to leaching.

Mineralization and organic carbon inputs to soil through root exudation and plant litter are tightly linked to the availability of other nutrients, in particular, nitrogen (Bengtson et al. 2012; Henriksen and Breland 1999;

Manzoni and Porporato 2009). Variations in soil water content can alter the microbial activity of the nitrogen cycle, and its overall effect on nitrogen losses may be different from that of carbon (Gu and Riley 2010; Schimel 2018). The available inorganic nitrogen produced by increased SOM mineralization after a rainfall pulse may be immobilized into microbial biomass (Dijkstra et al. 2012), taken up by plants (LLü et al. 2014), leached (Neilen et al. 2017), nitrified (Bateman and Baggs 2005; Stark and Firestone 1995), or lost as nitrogen gases through denitrification (Li et al. 1992; Sexstone et al. 1985; Riley and Matson 2000). Microbial activity and plant nitrogen uptake may also have different responses to increased drying-rewetting cycles (Collins 2008; Schwinning and Sala 2004) and the size of water pulses (Dijkstra et al. 2012). It is therefore difficult to predict the interactions and competitions between these processes, and estimating their feedback on the carbon cycle can be even more challenging.

Owing to experimental studies that showed rapid microbial response to soil moisture (Lundquist et al. 1999; Lee et al. 2004) and that soil microbes can resuscitate and become active within hours after a rewetting event (Placella et al. 2012; Barnard et al. 2015), we question if the intensification in hourly rainfall extremes can have a more significant impact on SOM dynamics than daily variations. To this end, we aim to quantify the long-term impacts of hourly and daily rainfall variations on carbon and nitrogen emissions, leaching, and storage in grasslands with different seasonal rainfall regimes using a mechanistic model. We coupled the BAMS1 model developed in Riley et al. (2014) to the nitrogen cycle model developed in Maggi et al. (2008) by accounting for C and N stoichiometric compositions of various SOM pools. The C–N coupled model (called BAMS2; Biotic and Abiotic Model of SOM version 2) includes 11 SOM pools (four polymer pools and seven monomer pools), five microbial functional groups (heterotrophic fungi and bacteria, ammonia oxidisers, nitrite oxidisers, and denitrifiers), plant nitrogen uptake, microbial growth, mortality and decomposition, protection, aqueous advection and diffusion, gaseous diffusion, aqueous complexation, and gaseous dissolution. BAMS2 was first benchmarked against field-observed heterotrophic soil respiration; N_2O and NO emissions; organic carbon inputs; and plant nitrogen uptake reported in the literature, and was then used to conduct a suite of numerical experiments on different hourly and daily rainfall variations in nine Australian grasslands located in tropical, temperate, and semi-arid regions.

Methods

BAMS2 reaction network

To account for the control of nitrogen availability on SOM dynamics, the BAMS1 carbon model described in Riley et al. (2014) was coupled to the nitrogen cycle model developed in Maggi et al. (2008). The C–N coupled reaction network (BAMS2, Fig. 1) consists of four SOM polymer pools (lignin, cellulose, hemicellulose, peptidoglycan); seven SOM monomer pools (monosaccharide, fatty acids, organic acids, phenols, nucleotides, amino acids, amino sugars); seven inorganic nitrogen molecules (NH_3, NH_4^+, NO_3^-, NO_2^-, NO, N_2O, N_2); and five microbial functional groups including heterotrophic fungi (F_{DEP}), heterotrophic bacteria (B_{HET}), ammonia-oxidizing bacteria (B_{AOB}), nitrite-oxidizing bacteria (B_{NOB}), and denitrifying bacteria (B_{DEN}).

In BAMS2, NH_4^+ is a substrate in SOM decomposition reactions (R1–R8 in Fig. 1). All microbial functional groups assimilate both carbon and nitrogen for growth, with fungi and bacteria having a C:N ratio of 8 and 5, respectively (Mouginot et al. 2014). In the mineralization of N-containing monomers (R9–R11), a fraction of mineralized nitrogen is assimilated into microbial biomass and the other fraction is released to the environment as free NH_4^+, which can be used by F_{DEP} and B_{HET} to decompose SOM, oxidized by B_{AOB} to NO_2^-, and taken up by plants. The original stoichiometric parameters of SOM decomposition reactions in BAMS1 (Riley et al. 2014) were recalculated to account for the nitrogen immobilization into microbial biomass (Supplementary Information Table S.1).

Similarly, the stoichiometric parameters of nitrification (R12–R13) and denitrification (R14–R17) reactions reported in Maggi et al. (2008) were recalculated to account for both carbon and nitrogen assimilation into microbial biomass (Supplementary Table S.1). In addition to nitrification and denitrification, BAMS2 includes N_2 fixation to NH_4^+ (R19). Although R19 represents biological fixation, the N_2 fixing microbial functional group is not explicitly accounted for because N_2 fixing microbes have a wide range of metabolic requirements; for example, they can be either aerobic or anaerobic and can be either heterotrophic, autotrophic, chemolithotrophic, or methanogenic (Reed et al. 2011).

Plants uptake both NH_4^+ and NO_3^- (R20–R21) and produce aboveground (R28–R29, leaf and wood litter with C:N ratio of 35, Moretto et al. 2001; Thomas and Asakawa 1993) and belowground (R27, root exudates with C:N

ratio of 12, Grayston et al. 1997; Mench and Martin 1991) SOM inputs. Litter decomposes into simpler organic polymers and monomers through implicit exoenzyme activity (Riley et al. 2014), while root exudates contain only organic monomers such as monosaccharide, fatty acids, organic acids, and amino acids (Grayston et al. 1997). The carbon and nitrogen assimilated into microbial biomass are returned to the SOM pools through microbial mortality (R22–R26). Here, microbial mortality and necromass decomposition are modeled as one lumped process.

In addition to biological processes, SOM monomers and inorganic nitrogen also undergo abiotic processes such as advection and diffusion, gas dissolution (R41–R45), and protection (e.g., via mineral surface binding, R30–R39). SOM polymers are considered to be non-soluble (in solid phases) organic carbon and do not undergo protection processes.

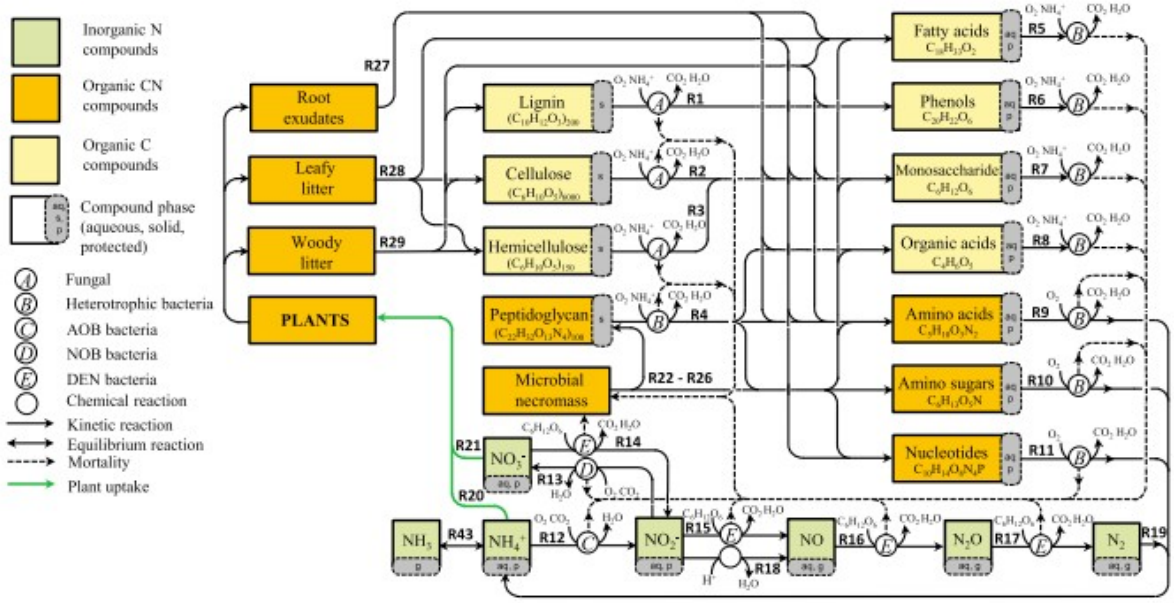

Fig. 1 C–N coupled reaction network described in BAMS2

Biogeochemical and transport solver

The BAMS2 reaction network (Fig. 1) was solved in the general-purpose multi-phase and multi-component bioreactive transport simulator BRTSim-v3.1a (Maggi 2019). BRTSim solves for the mass continuity and conservation laws using hybrid explicit-implicit finite volumes solvers. The water flow along a one-dimensional variably saturated soil column is modeled using the Richards equation (Richards 1931) in conjunction with the empirical relative permeability-potential-saturation relationship of the Brooks-Corey model (Brooks and Corey 1964). The transport of dissolved compounds is described by the Darcy's advection velocity and the Fick's diffusion. The advection of

gaseous compounds is excluded, but gas diffusion is explicitly accounted for using Fick's law. Equations used to model the transport of fluids and compounds in aqueous, gaseous, and biological phases are described in detail in Maggi (2019).

Aqueous complexation and gas dissolution (R40–R45, Supplementary Table S.1) are described in BRTSim-v3.1a using the mass action law (Maggi 2019),

$$K = \prod_R [\mathrm{X}_R]^{-x_R} \cdot \prod_P [\mathrm{X}_P]^{x_P}, \quad (1)$$

where K is the equilibrium constant, $[\mathrm{X}_R]$ and $[\mathrm{X}_P]$ are the reactant and product concentrations, respectively, with x_R and x_P their corresponding stoichiometric parameters. The values of K used in R40–R45 are obtained from Wolery (1992). Units for all variables are given in Supplementary Table S.2.

Chemical protection (R30–R39) is described using Langmuir kinetics to account for the protective capacity of soil, such that (Atkins and De Paula 2005),

$$\frac{\mathrm{d}[\mathrm{X(p)}]}{\mathrm{d}t} = k_a(Q_{max} - [\mathrm{X(p)}])[\mathrm{X(aq)}] - k_d[\mathrm{X(p)}], \quad (2)$$

where [X(p)] and [X(aq)] are the concentrations of chemical X in protected (p) and aqueous (aq) phases, respectively; k_a and k_d are the forward (protection) and reverse (un-protection) rate constants, respectively; and Q_{max} is the maximum soil protective capacity. At equilibrium ($\mathrm{d}[\mathrm{X(p)}]/\mathrm{d}t = 0$), $K_P = k_a/k_d$ is the protection equilibrium constant. Eq. 2 describes protection as a function of silt and clay content through the variable Q_{max}. For SOM protection, Q_{max} is estimated using the empirical relationship derived in Six et al. (2002) , i.e., Q_{max} [g-C protected kg soil^{-1}] $=0.32\times C_{fine}[\%]+16.33$, where C_{fine} is the silt and clay content. For $\mathrm{NH_4^+}$ protection, Q_{max} [g-$\mathrm{NH_4^+}$-N protected kg soil^{-1}] $=20.07\times C_{fine}[\%]$ (Alshameri et al. 2018) is used, while Q_{max} [g-$\mathrm{NO_3^-}$/$\mathrm{NO_2^-}$-N protected kg soil^{-1}] $=4.73\times10^{-4}\times C_{fine}[\%]$ (Black and Waring 1979) is used for the protection of $\mathrm{NO_3^-}$ and $\mathrm{NO_2^-}$.

Chemical and biochemical kinetic reactions are solved using the general framework of Michaelis–Menten–Monod kinetics described in Maggi and Riley

(2010). A biochemical kinetic reaction involving growth of microbial functional group B_X can be written as,

$$R = kf_S \frac{[B_X]}{Y} \prod_i \frac{[\mathrm{X}_i]}{[\mathrm{X}_i] + K_{M_i}} \prod_m \frac{K_{I_m}}{K_{I_m} + [\mathrm{X}_m]}, \qquad (3)$$

where R is the reaction rate; k is the reaction rate constant; f_S is the biological activity-moisture response function accounting for water stress; Y is the biomass yield; $[\mathrm{X}_i]$ is the concentration of reactant X_i with K_{Mi} its Michaelis–Menten half saturation; and $[\mathrm{X}_m]$ is the concentration of inhibitor X_m with K_{Im} the inhibition constant. In addition to carbon and nitrogen sources, O_2(aq) is a reactant in all aerobic reactions, while it is an inhibitor in anaerobic reactions. Microbial dynamics is described using Monod kinetics (Monod 1949),

$$\frac{\mathrm{d}[B_X]}{\mathrm{d}t} = \sum_i Y_i R_i - \delta[B_X], \qquad (4)$$

where δ is the microbial mortality rate constant.

Interactions between microbes and soil moisture are complex; in water-limiting conditions, microbial activity and growth are decreased due to increased physiological stress, reduced substrate diffusion towards microbes, and increased substrate adsorption to soil (Schimel et al. 2007; Manzoni et al. 2016; Yan et al. 2016). Although several studies have attempted to mechanistically describe these interactions through complex mathematical formulations (Davidson et al. 2012; Moyano et al. 2013; Manzoni et al. 2016), and more recently through reduced order approaches to time-scale respiration coefficient (Yan et al. 2018) and scaling arguments (Tang and Riley 2019), the microbial response to soil moisture is dealt with in this study using the liquid-biology feedback that defines f_S in Eq. 3 as (Maggi 2019)

$$f_S = \min\{f(S_B), f(S_L)/\max\{f(S_L)\}\}. \qquad (5)$$

The function $f(S_B)$ describes the immobilization of water into microbial biomass that has a specific water volume fraction f_L and considers water as a resource for microbial growth. Therefore, microbes can only grow if there is enough water to immobilize and enough pore space to occupy. When microbes die and decompose, water is re-mobilized and returned to the soil. Following the approach in Maggi and Porporato (2007), $f(S_B)$ is defined as

$$f(S_B) = \min\left\{1 - \frac{S_B - S_{Lr}}{1 - S_{Lr}}, 1 - \frac{f_L S_B}{S_L - S_{Lr}}, 1 - \frac{(1 - f_L)S_B}{S_G - S_{Gr}}\right\}, \quad (6)$$

where S_B, S_L, and S_G are the saturation in biological, liquid, and gaseous phases, respectively; and S_{Lr} and S_{Gr} are the residual saturation in liquid and gaseous phases, respectively. In this study, all microbial functional groups were assumed to have f_L=0.8. The function $f(S_L)$ in Eq. 5 describes the reduction of microbial activity as a result of changes in water saturation to account for processes not explicitly modeled, such as physiological stress and substrate diffusion within a soil layer; note that chemical transport across soil layers is explicitly modeled as described above. Finally, the function $f(S_L)$ in Eq. 5 is defined as

$$f(S_L) = \frac{S_L}{S_{L,LB} + S_L} \frac{S_{L,UB}}{S_{L,UB} + S_L}, \quad (7)$$

where $S_{L,LB}$ and $S_{L,UB}$ are scalar parameters. $S_{L,LB} = S_{L,UB}$ =0.46, estimated from experimental data in Wickland and Neff (2008) (Supplementary Fig. S.1a), are used in all microbial mediated kinetic reactions.

Active plant uptake of NH_4^+ and NO_3^- is described by Michaelis–Menten kinetics as

$$R_{N_{plant}} = f_S \left(k_{NH_4^+} \frac{[NH_4^+]}{[NH_4^+] + K_{M_{NH_4^+}}} + k_{NO_3^-} \frac{[NO_3^-]}{[NO_3^-] + K_{MNO_3^-}} \right), \quad (8)$$

where R_{Nplant} is the plant nitrogen uptake rate; $k_{NH_4^+}$ and $k_{NO_3^-}$ are rate constants; and $K_{M_{NH_4^+}}$ and $K_{M_{NO_3^-}}$ are Michaelis–Menten constants for NH_4^+ and NO_3^- uptake, respectively. The total amount of nitrogen taken up by plants (N_{plant}) is used to regulate SOM inputs (see R27–R29, Supplementary Table S.1) in such a way that the total amount of organic N input to soil is always smaller than or equal to N_{plant}. Hence, in instances when plant nitrogen uptake is low, the inputs of SOM will also be low. Because plants also

experience water stress in dry conditions (Manzoni and Porporato 2007; Porporato et al. 2003), a reduction factor of $f_S=f(S_L)/\max\{f(S_L)\}$ (Supplementary Fig. S.1b) is used in Eq. 8.

A summary of model parameters is reported in Table S.1, and a list of inhibitions applied to each kinetic reaction is reported in Supplementary Table S.3. Descriptions of mathematical equations, numerical methods, and solution convergence criteria used in BRTSim-v3.1a are detailed in Maggi (2019). An example of the input files for BAMS2 model is provided along with the Supplementary Information and the BRTSim solver can be downloaded from the links provided in the Acknowledgments.

Site descriptions

The BAMS2 reaction network was applied in nine Australian grasslands in tropical, temperate, and semi-arid regions that have distinct seasonal rainfall regimes. Site locations were determined based on the Dynamic Land Cover Dataset (Lymburner et al. 2011) and the modified KOppen climate classification of the Bureau of Meteorology, Australia (Stern and Dahni 2013) (Table 1). The tropical region is characterized by a pronounced dry season starting from May to September and is followed by a period of heavy rainfall between October and April with an average annual rainfall of 1289 mm y^{-1} (Supplementary Fig. S.2). In contrast, the wet season in the temperate region starts from May to September with lower annual rainfall but a higher number of wet days than the tropical region. The semi-arid region generally has low annual rainfall with a small number of wet days (Table 1).

Soil characteristics at each site were obtained from the SoilGrids database (Hengl T et al. 2017) and were used to estimate the hydraulic parameters (Supplementary Table S.4). The reactive transport model described in “BAMS2 reaction network” and “Biogeochemical and transport solver” sections was solved over a 2 m soil column with constant saturation as the lower boundary condition. Water boundary fluxes entering and leaving the soil column were defined by rainfall and plant evapotranspiration (Supplementary Fig. S.2). Historical daily rainfall and temperature data (from 1979 to 2017) at each site were obtained from the CPC US Unified Precipitation data provided by the NOAA/OAR/ESRL PSD, Boulder, Colorado, USA (Xie et al. 2010), and the Global Historical Climatology Network-Daily dataset (Menne et al. 2012), respectively. The Richardson-type weather generator developed by Chen et al. (2010) was then used to produce 2000-year daily rainfall and temperature time series with statistical properties similar to those of historical data. Plant actual evapotranspiration (ET) is calculated as $ET=k_c\times ET_0$ with the plant coefficient $k_c=0.8$ (Allen et al. 2005) and the potential evapotranspiration ET_0 estimated using the FAO ET_O

calculator (Allen et al. 1998). The root density along the soil profile is assumed here to be a negative exponential distribution function with 50% of root density located at 0.1 m (Christie 1978; Greenwood and Hutchinson 1998). Plant water uptake (evapotranspiration), plant nitrogen uptake (R20–R21), and root exudation (R27) were allocated over the soil depth according to the root distribution.

Table 1 Summary of site locations and climatic characteristics

Site ID	Latitude (°)	Longitude (°)	Climate[a]	Land cover[b]	Rainfall[c] (mm y^{-1})	No. of wet days y^{-1} [c]	T_{max} [d] (°C)	T_{min} [d] (°C)
TR1	−15.8478	141.7338	Tropical	Grassland	1223.2	141	38.81	10.86
TR2	−13.2052	132.0677	Tropical	Grassland	1448.7	174	38.07	11.85
TR3	−14.3539	126.7190	Tropical	Grassland	1195.7	146	39.83	10.75
TE1	−35.7914	137.9730	Temperate	Grassland	490.9	217	35.85	3.30
TE2	−33.8202	135.2551	Temperate	Grassland	386.4	166	39.53	2.99
TE3	−34.4754	117.3441	Temperate	Grassland	557.6	233	38.05	2.52
SA1	−18.9368	130.6136	Semi-arid	Grassland	608.9	110	42.74	4.50
SA2	−29.4720	144.9519	Semi-arid	Grassland	328.3	89	43.23	2.00
SA3	−29.3240	120.2663	Semi-arid	Grassland	295.4	109	42.95	1.63

[a]Based on the modified KÖppen climate classification of Bureau of Meteorology, Australia (Stern and Dahni 2013)

[b]Based on the Dynamic Land Cover Dataset (Lymburner et al. 2011)

[c]Based on the CPC US Unified Precipitation data provided by the NOAA/OAR/ESRL PSD, Boulder, Colorado, USA (Xie et al. 2010)

[d]Based on the Global Historical Climatology Network-Daily dataset (Menne et al. 2012b)

Rainfall scenarios

Numerical experiments were conducted with three rainfall scenarios. The weather generator in Chen et al. (2010) was modified to generate rainfall time series with varying statistical properties specific for each scenario, whereas no modification was applied to the evapotranspiration time series. We discuss the possible implication of this simplification below.

Scenario 1: change in annual cumulative rainfall amount. Rainfall time series were modified so that the annual cumulative rainfall amount (P_{cum}) ranged within +/- 20% of the historical value, while the annual number of wet days (D_{wet}) remained constant. In this scenario, the rainfall magnitude P in each quantile and the annual maximum daily rainfall (R_d^{max}) changed linearly with changes in P_{cum}, i.e., a 20% increase in P_{cum} led to 20% increases in P in all quantiles and R_d^{max} (Supplementary Fig. S.3, first row).

Scenario 2: change in daily rainfall amount and frequency. Rainfall time series were modified for D_{wet} to range within +/- 50% of the historical value while keeping P_{cum} unchanged. A decrease in D_{wet} caused a reduction in P at low quantiles and an increase in P at high quantiles, implying fewer and

heavier rainfalls. Percent change in R_d^{max} increased non-linearly with decreasing D_{wet}; for example, a 50% decrease in D_{wet} resulted in a 70% increase in R_d^{max} (Supplementary Fig. S.3, second row).

Scenario 3: change in hourly rainfall. Hourly rainfall time series were constructed by exponentially distributing the observed daily rainfall to a given number of wet hours H_{wet} in that day. Here, we used H_{wet}=24 hours as the reference and we generated hourly rainfall time series with decreasing H_{wet} by assuming the probability to rain in a given hour is independent of the hour before. Hourly rainfall intensified with decreasing H_{wet} (Supplementary Fig. S.3, third row).

Analyses and benchmarking

Prior to the numerical experiments, baseline simulations (using historical rainfalls) were initialized with SOM concentrations close to the organic carbon content reported in the SoilGrids database (Hengl T et al. 2017) and the microbial biomass close to zero. The simulations were run for 2000 years for biochemical reactions in the root zone to reach a steady state and to develop a steady microbial biomass profile. For reporting our results, we considered the top 30 cm of the soil as the root zone (RZ). The outputs of the 2000-year simulations were then used as initial conditions in the numerical experiments. In all numerical experiments, simulations were run for 1000 years and outputs from the last 50 years of simulation were averaged for analysis.

Baseline simulations were benchmarked against field observations collected from the literature with benchmark values reported in Table 2. Because BAMS2 includes only microbial heterotrophic respiration, CO_2 emissions in the baseline simulations were compared against heterotrophic soil respiration flux (R_H) of 353 natural and unmanaged grasslands reported in the Soil Respiration Database Version 4.0 (SRDB-V4 Bond-Lamberty and Thomson 2018). In instances where the values of R_H were not reported, we assumed that the ratio between heterotrophic and autotrophic respiration is 1:1, i.e., R_H=0.5R_s, with R_s as the total carbon flux from soil respiration. N_2O emissions were benchmarked against measurements in 40 grasslands reported in the database of Aronson and Allison (2012), while NO emissions were compared against the dataset reported in Davidson and Kingerlee (1997). The annual carbon inputs were compared against observations in 46 grasslands recorded in the Global Database of Litterfall Mass and Litter Pool Carbon and Nutrients (Holland et al. 2015), whereas the annual plant nitrogen uptake was benchmarked against field experiments of 16 grass species reported in Bessler et al. (2012).

The correlation between two quantities x and y is calculated as $R(x,y)= \mathrm{cov}(x,y)/\sigma_x\sigma_y$, where σ_x and σ_y are the standard deviations of x and y, respectively. The lag time between two time series was quantified using cross-correlation analysis (function *xcorr* in Matlab2017a).

Results

Benchmarking of baseline simulations

The modeled CO_2, N_2O, and NO emissions; SOM input rates; and plant nitrogen uptake rates were within the range of field measurements reported in various databases (Table 2). In baseline simulations, the semi-arid grasslands, which received the lowest amount and least frequent rainfall, had the lowest CO_2 emissions and SOM inputs (Fig. 2). Although the tropical grasslands had the highest depolymerization and SOM input rates, CO_2 emissions in these sites were slightly lower than those in the temperate grasslands. This pattern may be explained by the high denitrification rates in the temperate grasslands that contributed to CO_2 emissions and the slightly lower mineralization rates in the tropical grasslands. In all grasslands, the depolymerization rates were substantially lower than the mineralization of SOM monomers, suggesting that depolymerization is the rate-limiting process that controls CO_2 emissions.

NO and N_2O emissions were highest in the temperate and semi-arid grasslands, respectively (Fig. 2a). In the tropical grasslands, NO and N_2O emissions were either negative (i.e., a sink) or close to zero. Although some studies have observed negative N_2O fluxes (da Silva Cardoso et al. 2017) and low denitrification capacity (Xu et al. 2013) in tropical soils, other studies argued that a wetter soil would have higher anaerobicity, and therefore should have higher N_2O emissions (Skiba and Smith 2000). However, the process that limited N_2O and NO emissions in our tropical grassland simulations is nitrification rather than denitrification (Fig. 2b). In BAMS2, $\mathrm{NH_4^+}$ is the only source of inorganic nitrogen to the soil, mainly coming from N_2 fixation (R19) and mineralization of N-containing monomers (R9–R11). $\mathrm{NH_4^+}$ has to be first nitrified to $\mathrm{NO_2^-}$ or $\mathrm{NO_3^-}$ before B_{DEN} can further convert the nitrogen into NO and N_2O. In tropical grasslands, the soil water content was relatively high (i.e., soil saturation $S\approx0.6-0.8$), and therefore the $\mathrm{NH_4^+}$ concentration in the root zone was low. At low $\mathrm{NH_4^+}$, B_{AOB}, which has a high K_M value for $\mathrm{NH_4^+}$, was out-competed by B_{HET} and F_{DEP}. Because the

transformation of NH_4^+ to NO_3^- by B_{AOB} was suppressed, denitrification could not occur and led to negligible N_2O and NO emissions in the tropical grasslands. We note however that, in wet soils that have low NH_4^+ concentrations, the nitrifiers may have adapted to a K_M value lower than that applied in BAMS2, which was calibrated against temperate soils (Maggi et al. 2008).

Table 2 Model benchmark against field observations reported in the literature

Variables		BAMS2 modeled values	Values in the literature	References
CO_2 flux	Range	[18.34, 102.26]	[0.84, 1505]	Bond-Lamberty and Thomson (2018)
(g C m^{-2} y^{-1})	Mean ± σ	65.31 ± 32.36	397.48 ± 265.32	
N_2O flux	Range	[-5.1×10^{-4}, 171.48]	[− 13.33, 268.06]	Aronson and Allison (2012)
(mg N m^{-2} y^{-1})	Mean ± σ	102.68 ± 78.07	98.05 ± 91.63	
NO flux	Range	[-6.0×10^{-5}, 169.45]	[0, 292]	Davidson and Kingerlee (1997)
(mg N m^{-2} y^{-1})	Mean ± σ	91.56 ± 73.85	120.45 ± 18.25	
SOM inputs	Range	[20.86, 167.36]	[10.00, 835.00]	Holland et al. (2015)
(g C m^{-2} y^{-1})	Mean ± σ	97.14 ± 54.82	253.89 ± 181.42	
Plant N uptake	Range	[1.58, 12.26]	[<1, 20]	Bessler et al. (2012)
(g N m^{-2} y^{-1})	Mean ± σ	7.38 ± 4.03	11.4 ± 0.9	

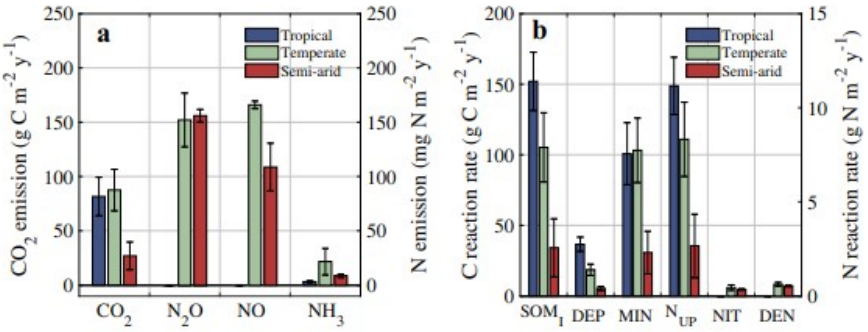

Fig. 2 **a** CO_2, N_2O, NO, and NH_3 emissions and **b** SOM inputs (SOM_I), depolymerization (DEP), monomer mineralization (MIN), plant nitrogen uptake (N_{UP}), nitrification (NIT), and denitrification (DEN) rates in tropical, temperate, and semi-arid grasslands under historical rainfall patterns. Error bars represent the standard deviations of the three sites in the same climatic region. Results are the averages of the last 50 years of the simulation period

Controls of soil moisture dynamics on C and N emissions

To better understand how soil moisture dynamics and daily rainfall impact carbon and nitrogen emissions, we analyzed the correlations (R) between time-series of soil saturation *S*; daily rainfall amount *P*; and CO_2, N_2O, NO, and NH_3 emissions (Fig. 3). In all grasslands, the correlation R(*S*, *P*) was relatively weak with slightly higher values observed in the tropical grasslands in the wet season. In general, *S* had a better correlation with C and N emissions as compared to *P*.

Simulations with BAMS2 were able to capture relatively well the *Birch effect* resulting from drying-rewetting cycles in the semi-arid and temperate grasslands, with a peak in CO_2 emission observed after rainfall events (Supplementary Fig. S.5). Except for SA1 that has a wet season between October to April (Supplementary Fig. S.2), SA2 and SA3 are relatively dry throughout the year and are considered to have only a dry season. CO_2, N_2O, and NO emissions in the semi-arid and temperate grasslands had relatively high positive correlations with *S* (R > 0.63, Fig. 3) during the dry season. The peaks in CO_2 came approximately five to six days after the peak in *S*, and N_2O and NO emissions came less than one day after the peak in *S* (Supplementary Fig. S.4). In the wet season, the correlations were slightly lower in the temperate grasslands and were substantially lower in the semi-arid grasslands.

In contrast to temperate and semi-arid grasslands, CO_2 emissions in the tropical grasslands were negatively correlated with *S* regardless of the season (Fig. 3, first row). In all grasslands, NH_3 emissions generally had high negative correlations with *S* during the dry season.

These correlation analyses suggest that soil moisture has an important control on greenhouse gas emissions in both high and low annual rainfall grasslands.

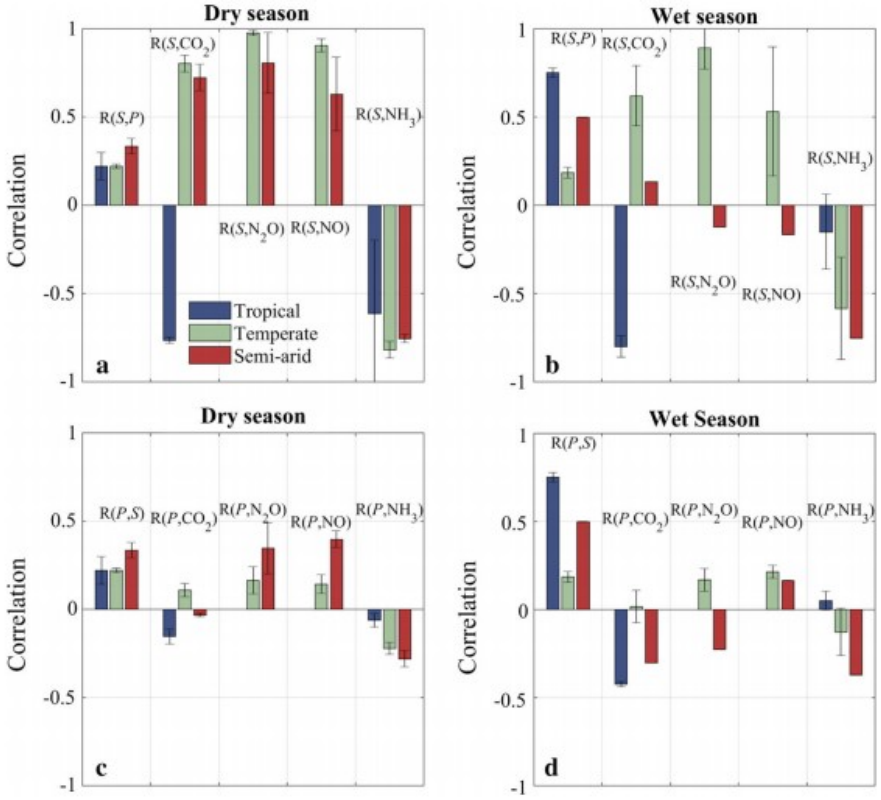

Fig. 3 Correlations of average soil saturation *S* in the root zone (first row) and daily rainfall amount *P* (second row) against CO_2, N_2O, NO, and NH_3 emissions in the dry and wet seasons. Error bars represent the standard deviations of the three sites in the same climatic region. Among the three semi-arid grasslands, only SA1 has a wet season

Scenario 1: impacts of annual rainfall amount

Contrary to the general expectation that increasing annual rainfall (P_{cum}) would have a larger impact on drier lands, our simulations suggested that both dry and wet grasslands are very sensitive to changes in P_{cum}, and they have distinctive responses (Fig. 4).

In the semi-arid grasslands, all carbon and nitrogen emissions increased by 10% to 30% when P_{cum} was increased by 20% (Fig. 4a–d). An increase in water availability in the semi-arid grasslands increased all biological processes, including plant nitrogen uptake (Supplementary Fig. S.7f), SOM inputs to soil (Fig. 4h), heterotrophic respiration (Fig. 4f, g), nitrification (Supplementary Fig. S.7d), and denitrification (Supplementary Fig. S.7e). The increased biological activity, however, increased only slightly the SOM stocks (<5%<5%, Fig. 4e). Together with increased water advection at high P_{cum}, the increased biological activity also led to a substantial increase in DOC and DIC leaching to soils below the root zone (Supplementary Fig. S.7a, b).

CO_2 emissions in the temperate grasslands increased by less than 3% with increasing P_{cum} (Fig. 4a). Depolymerization and mineralization rates increased only slightly with increased water availability, but this was associated with a higher increase in SOM inputs, hence, resulting in SOM stocks approximately 10% greater than those in the baseline simulations (Fig. 4). Although heterotrophic respiration was enhanced with increasing soil water, nitrification and denitrification rates in the temperate grasslands decreased substantially with increasing P_{cum}, leading to the reduction in N_2O and NO emissions (Fig. 4b, c). The increased water content may have diluted the concentration of NH_4^+ in the root zone, causing the nitrifiers and denitrifiers to be out-competed by heterotrophic bacteria and fungi. Increased water content also decreased the volatilization of ammonia (Fig. 4d).

In contrast to the semi-arid and temperate grasslands, the wet tropical grasslands generally featured a decrease in biological activity with increasing P_{cum}. CO_2 emissions decreased with increasing soil water content (Fig. 4a) because high water content reduced oxygen availability and decreased SOM and NH_4^+ concentrations, leading to decreasing heterotrophic respiration. In particular, the mineralization rates decreased two times more than the depolymerization (Fig. 4f, g) because the soluble SOM monomers tended to be advected out of the root zone at high P_{cum}. An increasing P_{cum} also reduced plant nitrogen uptake (Supplementary Fig. S.7f) and SOM inputs (Fig. 4h), but the overall balance between inputs and

decomposition resulted in a net SOM storage (Fig. 4e). Although DOC leaching increased with increasing soil water content, the decreased biological activity had substantially reduced the DIC leaching (Supplementary Fig. S.7a, b).

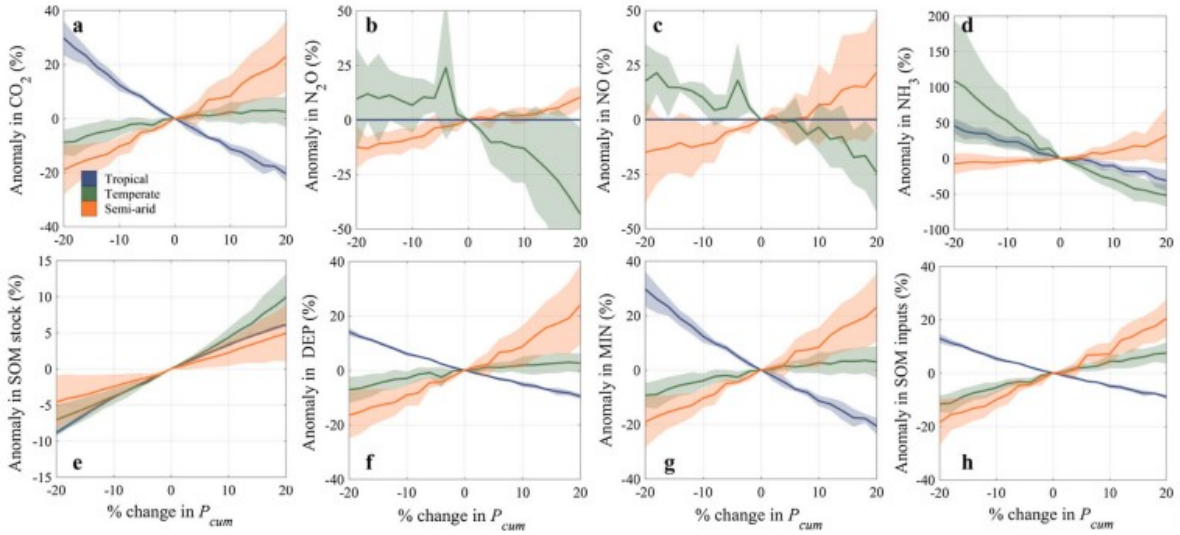

Fig. 4 Effects of changes in annual cumulative rainfall amount P_{cum} (Scenario 1) on annual **a** CO_2 emissions, **b** N_2O emissions, **c** NO emissions, **d** NH_3 emissions, **e** SOM stocks, **f** depolymerization rates (DEP), **g** mineralization rates of SOM monomers (MIN), and **h** SOM inputs rates. Shaded areas represent the standard deviations

Scenario 2: impacts of daily rainfall amount and frequency

We investigated the response of C and N dynamics to variations in daily rainfall amount and frequency by changing the number of wet days D_{wet} in a year while keeping the total annual rainfall constant; that is, a time-series with a smaller D_{wet} value has fewer but larger rainfall events.

Among all grasslands, the semi-arid grasslands were the most sensitive to variations in D_{wet}. CO_2 emissions in the semi-arid grasslands increased by approximately 7% with a 50% decrease in D_{wet} (Fig. 5a). Fewer and larger rainfall events increased the plant nitrogen uptake (Supplementary Fig. S.8f), and therefore increased the SOM inputs to soil (Fig. 5h). Upon the assumption that plant nitrogen uptake is proportional to plant biomass growth, similar experimental observations were reported in Heisler-White (2008) that showed an increase in aboveground net primary productivity when semi-arid ecosystems were subjected to rainfall events that were larger in size but fewer in number. The balance between increased SOM inputs and decomposition caused a slight increase in SOM stocks (<2%, Fig. 5e) and a substantial increase in DOC and DIC leaching to below the root zone (Supplementary Fig. S.8a, b). In contrast to SOM depolymerization and mineralization, the nitrification and denitrification rates in the semi-arid

grasslands were reduced with decreasing D_{wet}, leading to a reduction in N_2O emissions (Fig. 5b). Although biological denitrification was reduced, chemodenitrification increased with decreasing D_{wet} and contributed to the increasing NO emissions (Fig. 5c). The effects of increased rainfall intensity and reduced frequency on nitrogen emissions in the semi-arid grasslands matched relatively well with the numerical-experiments tested in Gu and Riley (2010). Gu and Riley (2010) also found that, when applied with a low total rainfall amount, high intensity and low frequency rainfall events reduced N_2O emissions in sandy loams soils, but increased NO emissions.

Less frequent and more intense events did not alter CO_2 emissions in the temperate grasslands but substantially reduced N_2O and NO emissions (Fig. 5a–c). Big pulses of water diluted and transported inorganic nitrogen out of the root zones, and hence decreased the nitrification and denitrification rates.

In the tropical grasslands, CO_2, N_2O, and NO emissions were not sensitive to the decrease in D_{wet}, but the NH_3 volatilization was greatly reduced (Fig. 5a–d). CO_2 emissions, however, increased slightly with increasing D_{wet}, suggesting that more frequent and less intense rainfall events can increase heterotrophic respiration in grasslands with tropical rainfall regimes.

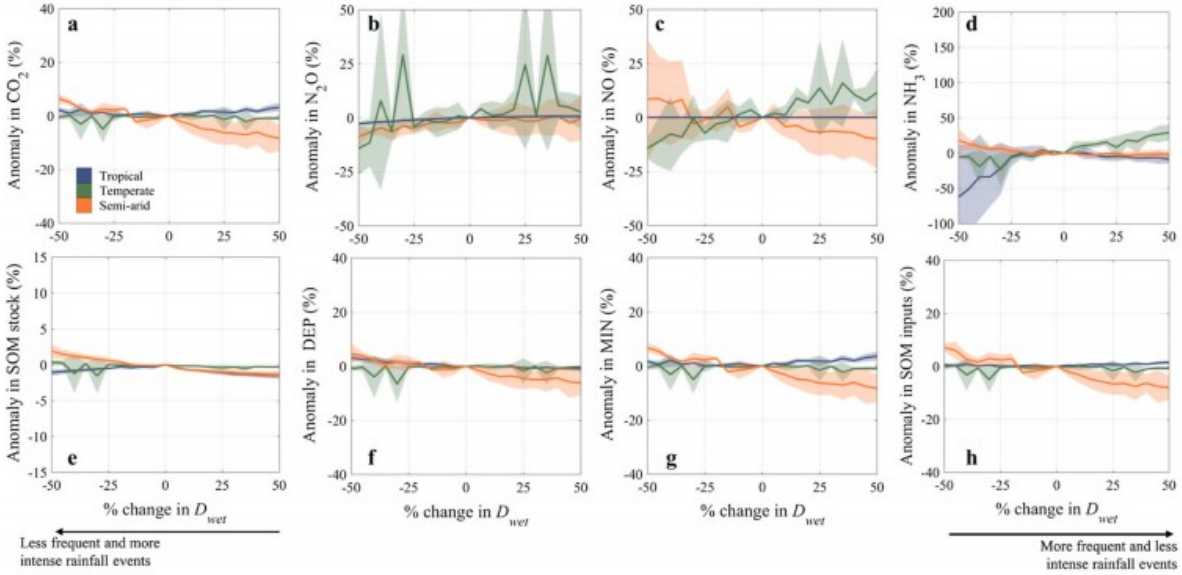

Fig. 5 Effects of changes in the number of wet days D_{wet} (Scenario 2) on annual **a** CO_2 emissions, **b** N_2O emissions, **c** NO emissions, **d** NH_3 emissions, **e** SOM stocks, **f** depolymerization rates (DEP), **g** mineralization rates of SOM monomers (MIN), and **h** SOM inputs rates. Shaded areas represent the standard deviations.

Scenario 3: impacts of hourly rainfall intensification

CO_2 emissions, SOM decomposition rates, and SOM stocks were relatively insensitive to hourly rainfall amounts in all grasslands with CO_2 emissions

increased only slightly in the tropical and semi-arid grasslands (<2%, Fig. 6a, e–g). DOC and DIC leaching to below the root zone, however, increased with a decreasing number of wet hours H_{wet} in the semi-arid grasslands (Supplementary Fig. S.9a, b).

Although SOM decomposition was not significantly affected, fewer and larger hourly rainfall events (i.e., decreasing H_{wet}) altered substantially the emissions of nitrogen gases. In the tropical grasslands, the NH_3 volatilization was largely reduced (i.e., >300% reduction, Fig. 6d) with decreased H_{wet}. In the temperate grasslands, denitrification rates slightly decreased with decreasing H_{wet} and caused a decline in N_2O and NO emissions (Fig. 6b, c). Although the denitrification rates were not substantially altered, the variation in hourly rainfall amounts changed the ratio of N_2O:NO production in the semi-arid grasslands (Fig. 6b, c), with N_2O:NO ratio increased as H_{wet} decreased.

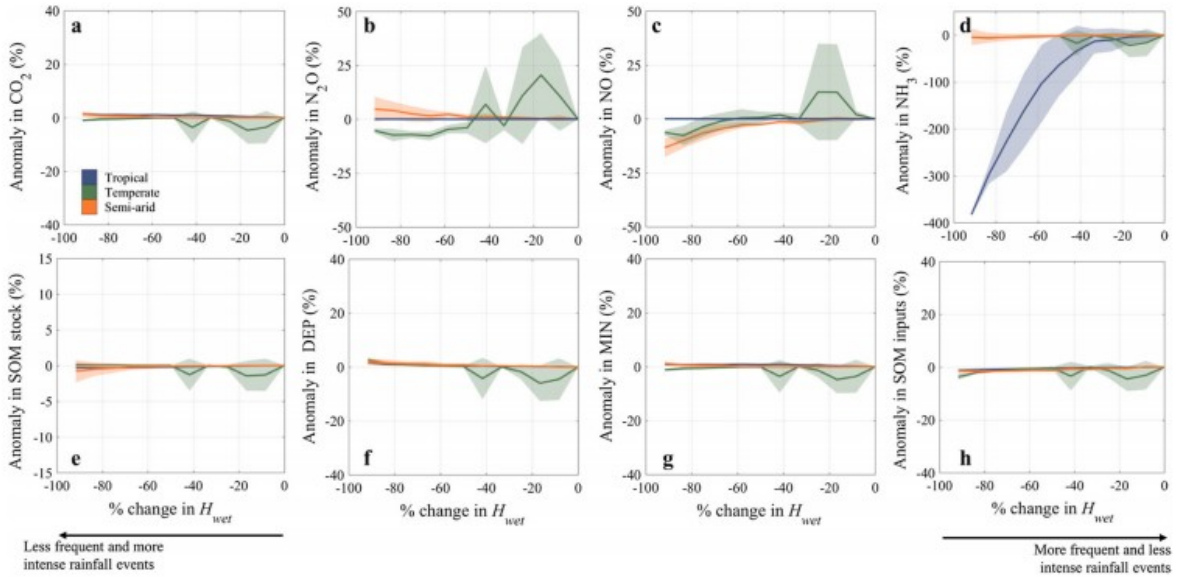

Fig. 6 Effects of changes in the number of wet hours H_{wet} (Scenario 3) on annual **a** CO_2 emissions, **b** N_2O emissions, **c** NO emissions, **d** NH_3 emissions, **e** SOM stocks, **f** depolymerization rates (DEP), **g** mineralization rates of SOM monomers (MIN), and **h** SOM inputs rates. Shaded areas represent the standard deviations

Discussion

The BAMS2 model represents the highly complex interplay between many biotic and abiotic mechanisms hypothesized to be important for carbon and nitrogen cycles, including depolymerization, SOM mineralization, microbial mortality, necromass decomposition, N_2 fixation, nitrification, denitrification, protection, advection, and diffusion. These mechanisms have different responses to soil water content, and therefore a detailed description of their interactions is pivotal to this study that explicitly aims at assessing the impact of rainfall variability on soil carbon and nitrogen dynamics. We note

however that the determination of model parameter values can be difficult for a model with high complexity, and this can introduce additional uncertainties. In this work, we used the *validation by construct* approach (McCarl and Apland 1986) to design and test our model. The model parameters relative to the carbon cycle were estimated against 618 SOM profiles of grasslands located across Nebraska and Colorado (detailed in Riley et al. 2014); those corresponding to the nitrification and denitrification processes were estimated against field measurements of CO_2, N_2O, and NO fluxes (detailed in Maggi et al. 2008); and the other parameters were estimated against field and laboratory experiments reported in the literature (detailed in Supplementary Table S.1). We then benchmarked the model outputs against field observed CO_2, N_2O and NO emissions; SOM inputs; and plant nitrogen uptake rates compiled in various databases (detailed in Table 2). Although the sensitivity analysis of model parameters had been conducted separately for carbon (Riley et al. 2014) and nitrogen (Maggi et al. 2008) cycles, we note that the parameter sensitivity may change after coupling the two models, and therefore a global sensitivity analysis of BAMS2 is needed, and it is the target of our next work.

Although the reaction network in BAMS2 is comparably or more complex than many other SOM models, there are still some other mechanisms that are currently not accounted for here. In BAMS2, we considered a simplified nitrogen cycle that includes only N_2 fixation, nitrification, and denitrification. However, the nitrogen cycle in soil is much more complicated than that, and many new metabolic capabilities of N-transforming microorganisms are continuously being discovered (Kuypers et al. 2018; Schreiber et al. 2012). Biotic N-transformation pathways not considered in BAMS2 include dissimilatory nitrate reduction to ammonium (DNRA, $\mathrm{NO_3^- \rightarrow NO_2^- \rightarrow NH_4^+}$, Tiedje et al. 1983), anaerobic ammonium oxidation (anammox, $\mathrm{NO_2^- \rightarrow NO + NH_4^+ \rightarrow N_2H_4 \rightarrow N_2}$, Mulder et al. 1995), complete ammonia oxidation (comammox, $\mathrm{NH_4^+ \rightarrow NO_3^-}$, Daims et al. 2015), hydroxylamine oxidation to nitric oxide ($\mathrm{NH_2OH \rightarrow NO}$, Caranto and Lancaster 2017), and nitric oxide dismutation to dinitrogen ($NO \rightarrow N_2$, Ettwig et al. 2010). We note that B_{AOB} and B_{NOB} can also reduce $\mathrm{NO_2^-}$ to NO and N_2O (Schreiber et al. 2012); however, this capability was not included in BAMS2. Even though complex, accounting for a more detailed description of the nitrogen cycle may improve the estimation of greenhouse gas emissions and SOM stocks as our simulation analysis shows that the interactions between soil carbon and nitrogen cycles have non-linear responses to rainfall variability.

By having fixed C:N ratios of litter and root exudates, we used a simplified approach to regulate the above- and belowground SOM inputs through plant nitrogen uptake in such a way that the total organic nitrogen inputs to the soil cannot exceed the total inorganic nitrogen (NH_4^+ and NO_3^-) taken up by plants. This approach assumes that all nitrogen taken up by plants is assimilated into plant biomass and eventually returned to the soil. The assimilation of carbon into plant biomass was not explicitly modeled, and hence we did not consider a dynamic litter C:N ratio. Improvements to the description of plant-soil interactions in BAMS2 may be implemented in future work to account for plant carbon assimilation, flexible C:N ratios for litter and root exudates, and the effects of nutrient limitation on photosynthesis capacity following suggestions in Achat et al. (2016).

We observed in our simulations that, when switching to a new rainfall pattern, the microbial population took a few decades to reach a steady profile and a steady bacterial to fungal ratio. This observation aligns with experimental studies that showed the dependency of soil respiration on historical rainfall, which can be explained by the shift in microbial community composition and activity (Lau and Lennon 2012; Hawkes et al. 2017). Hence, field studies that spanned across time-scales of months may capture only the transient effects. Although limited by the need to simplify an ecosystem, long-term simulations with models such as BAMS2 allow assessment of cumulative impacts of rainfall variability on soil C and N dynamics and identification of interactions between C and N cycles, which are difficult to capture in field studies. In particular, our simulations featured a tight link between soil respiration and nitrogen availability. Aligned with field data analysis in Wang and Fang (2009), we observed a reduction in CO_2 emissions with increasing annual rainfall in wet tropical grasslands, and we can explain this observation as a consequence of N limitation. Although increased rainfall amount releases plants and soil microbes from water stress, high soil water content also reduces the concentrations of inorganic N, putting soil microbes in an N-limiting condition and causing decreased soil respiration. In dry semi-arid grasslands, the observed increase in soil respiration with increasing rainfall amount can be attributed to the direct moisture effect on soil microbes that increases microbial activity and the indirect effect through increased plant litter (Lau and Lennon 2012). While the short-term impacts of drying and rewetting cycles on soil activity has been studied in many field experiments (e.g., Kieft 1987; Harper et al. 2005; Xiang et al. 2008), our simulations confirmed that, with no change in annual rainfall, prolonged droughts and increased high rainfall pulses can increase cumulative CO_2 emissions in dry grasslands in the long-term, which we attribute to increased

substrate availability as a result of accumulation (resulting from plant residuals and microbial lysis) during the droughts.

Conclusions

We present a C–N coupled mechanistic SOM model (BAMS2) to investigate the effects of hourly and daily rainfall variations on soil carbon and nitrogen emissions, stocks, and leaching in grasslands with different seasonal rainfall regimes. BAMS2 captured relatively well the *Birch effect* and the carbon and nitrogen dynamics observed in grasslands, with model outputs falling within the range of field observations compiled in various published databases. Dry and wet grasslands responded differently to variations in rainfall patterns and rainfall variability had a different impact on carbon and nitrogen emissions. An increasing annual rainfall generally increased both microbial and plant activities in the semi-arid grasslands, leading to increases in CO_2, N_2O, NO, and NH_3 emissions; yet, it reduced inorganic N availability in the tropical grasslands, decreased biological activities, and caused a reduction in CO_2 emissions. The balance between SOM inputs and decomposition, however, always resulted in increasing SOM stocks with increasing annual rainfall in all grasslands. High rainfall amounts can dilute NH_4^+ concentrations to below optimal values for nitrification, thus reducing N_2O and NO emissions in the temperate grasslands. Fewer and larger daily rainfall events slightly increased CO_2 emissions and SOM stocks in the semi-arid grasslands, but caused a substantial increase in NO emissions as a result of increased chemodenitrification. Changes in hourly rainfall amounts and frequency did not significantly alter soil carbon emissions and stocks in all grasslands. Although the biotic processes in the tropical grasslands are relatively insensitive to hourly rainfall variability, the high magnitude hourly rainfall events can substantially reduce NH_3 volatilization.

Acknowledgements

FHMT and FM are supported by the SREI2020 EnviroSphere research program of the University of Sydney. FM is also supported by the Mid Career Research Award and Sydney Research Accelerator Fellowship (SOAR) of the University of Sydney. WJR is supported by the Director, Office of Science, Office of Biological and Environmental Research of the U.S. Department of Energy under Contract No. DE-AC02-05CH11231 as part of the LBNL TES Belowground Biogeochemistry Scientific Focus Area. The authors thank Giulia Ceriotti for the many conversations on topics presented here. The authors acknowledge the Sydney Informatics Hub and the University of Sydney's high performance computing cluster Artemis for providing the high performance computing resources that have contributed to the results

reported within this work. The BRTSim solver package can be downloaded at https://sites.google.com/site/thebrtsimproject/home or from the mirror https://www.dropbox.com/sh/wrfspx9f1dvuspr/AAD5iA9PsteX3ygAJxQDxAy9a?dl=0.

References

Achat DL, Augusto L, Gallet-Budynek A, Loustau D (2016) Future challenges in coupled C–N–P cycle models for terrestrial ecosystems under global change: a review. Biogeochemistry 131(1–2):173–202

Allen RG, Pereira LS, Raes D, Smith M (1998) Crop evapotranspiration: guidelines for computing crop water requirements—FAO Irrigation and drainage paper 56. Food and Agriculture Organisation of the United Nations (FAO), Rome

Allen RG, Clemmens AJ, Burt CM, Solomon K, O'Halloran T (2005) Prediction accuracy for projectwide evapotranspiration using crop coefficients and reference evapotranspiration. J Irrig Drain Eng 131(1):24–36

Alshameri A, He H, Zhu J, Xi Y, Zhu R, Ma L, Tao Q (2018) Adsorption of ammonium by different natural clay minerals: characterization, kinetics and adsorption isotherms. Appl Clay Sci 159:83–93

Aronson E, Allison SD (2012) Meta-analysis of environmental impacts on nitrous oxide release in response to N amendment. Front Microbiol 3:272

Atkins P, De Paula J (2005) Elements of physical chemistry, 4th edn. Oxford University Press, Oxford

Barnard RL, Osborne CA, Firestone MK (2015) Changing precipitation pattern alters soil microbial community response to wet-up under a Mediterranean-type climate. ISME J 9(4):946

Bateman EJ, Baggs EM (2005) Contributions of nitrification and denitrification to N$_2$O emissions from soils at different water-filled pore space. Biol Fertil Soils 41(6):379–388

Bengtson P, Barker J, Grayston SJ (2012) Evidence of a strong coupling between root exudation, C and N availability, and stimulated SOM decomposition caused by rhizosphere priming effects. Ecol Evol 2(8):1843–1852

Bessler H, Oelmann Y, Roscher C, Buchmann N, Scherer-Lorenzen M, Schulze ED, Tempert VM, Wilcke W, Engels C (2012) Nitrogen uptake by grassland communities: contribution of N2 fixation, facilitation, complementarity, and species dominance. Plant Soil 358(1–2):301–322

Birch HF (1958) The effect of soil drying on humus decomposition and nitrogen availability. Plant Soil 10(1):9–31

Black AS, Waring SA (1979) Adsorption of nitrate, chloride and sulfate by some highly weathered soils from south-west Queensland. Soil Res 17(2):271–282

Bond-Lamberty BP, Thomson AM (2018) A Global Database of Soil Respiration Data, Version 4.0. ORNL DAAC, Oak Ridge, Tennessee, USA. https://doi.org/10.3334/ORNLDAAC/1578

Bouma TJ, Bryla DR (2000) On the assessment of root and soil respiration for soils of different textures: interactions with soil moisture contents and soil CO_2 concentrations. Plant Soil 227(1–2):215–221

Brooks RH, Corey AT (1964) Hydraulic properties of porous media. Hydrology Papers 3. Colorado State University, Fort Collins

Caranto JD, Lancaster KM (2017) Nitric oxide is an obligate bacterial nitrification intermediate produced by hydroxylamine oxidoreductase. Proc Natl Acad Sci 114(31):8217–8222

Chen J, Brissette FP, Leconte R (2010) A daily stochastic weather generator for preserving low-frequency of climate variability. J Hydrol 388(3–4):480–490

Christie EK (1978) Ecosystem processes in semiarid grasslands. I. Primary production and water use of two communities possessing different photosynthetic pathways. Aust J Agric Res 29(4):773–787

Collins SL, Sinsabaugh RL, Crenshaw C, Green L, Porras-Alfaro A, Stursova M, Zeglin LH (2008) Pulse dynamics and microbial processes in aridland ecosystems. J Ecol 96(3):413–420

Curiel Yuste J, Baldocchi DD, Gershenson A, Goldstein A, Misson L, Wong S (2007) Microbial soil respiration and its dependency on carbon inputs, soil temperature and moisture. Glob Chang Biol 13(9):2018–2035

Daims H, Lebedeva FV, Pjevac P, Han P, Herbold C, Albertsen M, Kirkegaard RH et al (2015) Complete nitrification by Nitrospira bacteria. Nature 528(7583):504

Davidson EA, Kingerlee W (1997) A global inventory of nitric oxide emissions from soils. Nutr Cycl Agroecosyst 48(1–2):37–50

Davidson EA, Samanta S, Caramori SS, Savage K (2012) The dual Arrhenius and Michaelis–Menten kinetics model for decomposition of soil organic matter at hourly to seasonal time scales. Glob Chang Biol 18(1):371–384

da Silva Cardoso A, de Figueiredo Brito L, Janusckiewicz ER, da Silva Morgado E, Barbero RP, Koscheck JFW, Ruggieri AC et al (2017) Impact of grazing intensity and seasons on greenhouse gas emissions in tropical grassland. Ecosystems 20(4):845–859

Delgado-Baquerizo M, Maestre FT, Gallardo A, Bowker MA, Wallenstein MD, Quero JL, García-Palacios P et al (2013) Decoupling of soil nutrient cycles as a function of aridity in global drylands. Nature 502(7473):672

Dijkstra FA, Augustine DJ, Brewer P, von Fischer JC (2012) Nitrogen cycling and water pulses in semiarid grasslands: are microbial and plant processes temporally asynchronous? Oecologia 170(3):799–808

Donat MG, Alexander LV, Yang H, Durre I, Vose R, Dunn RJH, Hewitson B et al (2013) Updated analyses of temperature and precipitation extreme indices since the beginning of the twentieth century: the HadEX2 dataset. J Geophys Res 118(5):2098–2118

Easterling DR, Meehl GA, Parmesan C, Changnon SA, Karl TR, Mearns LO (2000) Climate extremes: observations, modeling, and impacts. Science 289(5487):2068–2074

Ettwig KF et al, Butler MK, Le Paslier D, Pelletier E, Mangenot S, Kuypers MM, Gloerich J et al (2010) Nitrite-driven anaerobic methane oxidation by oxygenic bacteria. Nature 464(7288):543

Fischer EM, Knutti R (2014) Detection of spatially aggregated changes in temperature and precipitation extremes. Geophys Res Lett 41(2):547–554

Grayston SJ, Vaughan D, Jones D (1997) Rhizosphere carbon flow in trees, in comparison with annual plants: the importance of root exudation and its impact on microbial activity and nutrient availability. Appl Soil Ecol 5(1):29–56

Greenwood KL, Hutchinson KJ (1998) Root characteristics of temperate pasture in New South Wales after grazing at three stocking rates for 30 years. Grass Forage Sci 53(2):120–128

Gu C, Riley WJ (2010) Combined effects of short term rainfall patterns and soil texture on soil nitrogen cycling: a modeling analysis. J Contam Hydrol 112(1–4):141–154

Guerreiro SB, Fowler HJ, Barbero R, Westra S, Lenderink G, Blenkinsop S, Lewis E, Li XF (2018) Detection of continental-scale intensification of hourly rainfall extremes. Nat Clim Chang 8(9):803

Harper CW, Blair JM, Fay PA, Knapp AK, Carlisle JD (2005) Increased rainfall variability and reduced rainfall amount decreases soil CO$_2$ flux in a grassland ecosystem. Glob Chang Biol 11(2):322–334

Hawkes CV, Waring BG, Rocca JD, Kivlin SN (2017) Historical climate controls soil respiration responses to current soil moisture. Proc. Natl Acad. Sci. 114(24):6322–6327

Heisler-White JL, Knapp AK, Kelly EF (2008) Increasing precipitation event size increases aboveground net primary productivity in a semi-arid grassland. Oecologia 158(1):129–140

Hengl T, de Jesus JM, Heuvelink GB, Gonzalez MR, Kilibarda M, Blagotić A (2017) SoilGrids250m: global gridded soil information based on machine learning. PLoS ONE 12(2):e169748

Henriksen TM, Breland TA (1999) Nitrogen availability effects on carbon mineralization, fungal and bacterial growth, and enzyme activities during decomposition of wheat straw in soil. Soil Biol Biochem 31(8):1121–1134

Holland EA, Post WM, Matthews E, Sulzman J, Staufer R, Krankina O (2015) A global database of litterfall mass and litter pool carbon and nutrients. Data set. http://daac.ornl.gov from Oak Ridge National Laboratory Distributed Active Archive Center, Oak Ridge, Tennessee, USA https://doi.org/10.3334/ORNLDAAC/1244

Kieft TL (1987) Microbial biomass response to a rapid increase in water potential when dry soil is wetted. Soil Biol Biochem 19(2):119–126

Kim DG, Vargas R, Bond-Lamberty B, Turetsky MR (2012) Effects of soil rewetting and thawing on soil gas fluxes: a review of current literature and suggestions for future research. Biogeosciences 9(7):2459–2483

Kuypers MM, Marchant HK, Kartal B (2018) The microbial nitrogen-cycling network. Nat Rev Microbiol 16(5):263

Lau JA, Lennon JT (2012) Rapid responses of soil microorganisms improve plant fitness in novel environments. Proc Natl Acad Sci 109(35):14058–14062

Lee X, Wu HJ, Sigler J, Oishi C, Siccama T (2004) Rapid and transient response of soil respiration to rain. Glob Chang Biol 10(6):1017–1026

Li C, Frolking S, Frolking TA (1992) A model of nitrous oxide evolution from soil driven by rainfall events: 1. Model structure and sensitivity. J Geophys Res 97(D9):9759–9776

Li X, Miller AE, Meixner T, Schimel JP, Melack JM, Sickman JO (2010) Adding an empirical factor to better represent the rewetting pulse mechanism in a soil biogeochemical model. Geoderma 159(3–4):440–451

Liu T, Wang L, Feng X, Zhang J, Ma T, Wang X, Liu Z (2018) Comparing soil carbon loss through respiration and leaching under extreme precipitation events in arid and semiarid grasslands. Biogeosciences 15(5):1627–1641

Lü XT, Dijkstra FA, Kong DL, Wang ZW, Han XG (2014) Plant nitrogen uptake drives responses of productivity to nitrogen and water addition in a grassland. Sci Rep 4:4817

Lundquist EJ, Scow KM, Jackson LE, Uesugi SL, Johnson CR (1999) Rapid response of soil microbial communities from conventional, low input, and organic farming systems to a wet/dry cycle. Soil Biol Biochem 31(12):1661–1675

Lymburner L, Tan P, Mueller N, Thackway R, Lewis A, Thankappan M, Randall L, Islam A, Senarath U (2011) The National Dynamic Land Cover Dataset. Geoscience Australia. http://data.bioregionalassessments.gov.au/dataset/1556b944-731c-4b7f-a03e-14577c7e68db. Accessed 16 August 2018

Maggi F (2019) BRTSim, a general-purpose computational solver for hydrological, biogeochemical, and ecosystem dynamics. arXiv preprint arXiv:1903.07015

Maggi F, Porporato A (2007) Coupled moisture and microbial dynamics in unsaturated soils. Water Resour Res. https://doi.org/10.1029/2006WR005367

Maggi F, Riley WJ (2010) Mathematical treatment of isotopologue and isotopomer speciation and fractionation in biochemical kinetics. Geochim Cosmochim Acta 74(6):1823–1835

Maggi F, Gu C, Riley WJ, Hornberger GM, Venterea RT, Xu T, Oldenburg CM et al (2008) A mechanistic treatment of the dominant soil nitrogen cycling processes: model development, testing, and application. J Geophys Res. https://doi.org/10.1029/2007JG000578

Manzoni S, Porporato A (2007) A theoretical analysis of nonlinearities and feedbacks in soil carbon and nitrogen cycles. Soil Biol Biochem 39(7):1542–1556

Manzoni S, Porporato A (2009) Soil carbon and nitrogen mineralization: theory and models across scales. Soil Biol Biochem 41(7):1355–1379

Manzoni S, Schimel JP, Porporato A (2012) Responses of soil microbial communities to water stress: results from a meta-analysis. Ecology 93(4):930–938

Manzoni S, Moyano F, Kätterer T, Schimel J (2016) Modeling coupled enzymatic and solute transport controls on decomposition in drying soils. Soil Biol Biochem 95:275–287

Maslin M, Austin P (2012) Uncertainty: climate models at their limit? Nature 486(7402):183

McCarl BA, Apland J (1986) Validation of linear programming models. J Agric Appl Econ 18(2):155–164

Mench M, Martin E (1991) Mobilization of cadmium and other metals from two soils by root exudates of *Zea mays* L., *Nicotiana tabacum* L. and *Nicotiana rustica* L. Plant Soil 132(2):187–196

Menne MJ, Durre I, Vose RS, Gleason BE, Houston TG (2012) An overview of the global historical climatology network-daily database. J Atmos Ocean Technol 29(7):897–910

Menne MJ, Durre I, Korzeniewski B, McNeal S, Thomas K, Yin X, Anthony S, Ray R, Vose RS, Gleason BE, Houston TG (2012) Global historical climatology network—Daily (GHCN-Daily), Version 3. NOAA National Climatic Data Center. https://doi.org/10.7289/V5D21VHZ. Accessed September 2018

Monod J (1949) The growth of bacterial cultures. Annu Rev Microbiol 3(1):371–394

Moretto AS, Distel RA, Didoné NG (2001) Decomposition and nutrient dynamic of leaf litter and roots from palatable and unpalatable grasses in a semi-arid grassland. Appl Soil Ecol 18(1):31–37

Mouginot C, Kawamura R, Matulich KL, Berlemont R, Allison SD, Amend AS, Martiny AC (2014) Elemental stoichiometry of fungi and bacteria strains from grassland leaf litter. Soil Biol Biochem 76:278–285

Moyano FE, Manzoni S, Chenu C (2013) Responses of soil heterotrophic respiration to moisture availability: an exploration of processes and models. Soil Biol Biochem 59:72–85

Mulder A, Van de Graaf AA, Robertson LA, Kuenen JG (1995) Anaerobic ammonium oxidation discovered in a denitrifying fluidized bed reactor. FEMS Microbiol Ecol 16(3):177–183

Navarro-García F, Casermeiro MÁ, Schimel JP (2012) When structure means conservation: effect of aggregate structure in controlling microbial responses to rewetting events. Soil Biol Biochem 44(1):1–8

Neilen AD, Chen CR, Parker BM, Faggotter SJ, Burford MA (2017) Differences in nitrate and phosphorus export between wooded and grassed riparian zones from farmland to receiving waterways under varying rainfall conditions. Sci Total Environ 598:188–197

Nielsen UN, Ball BA (2015) Impacts of altered precipitation regimes on soil communities and biogeochemistry in arid and semi-arid ecosystems. Glob Chang Biol 21(4):1407–1421

Placella SA, Brodie EL, Firestone MK (2012) Rainfall-induced carbon dioxide pulses result from sequential resuscitation of phylogenetically clustered microbial groups. Proc Natl Acad Sci 109(27):10931–10936

Porporato A, Laio F, Ridolfi L, Caylor KK, Rodriguez-Iturbe I (2003) Soil moisture and plant stress dynamics along the Kalahari precipitation gradient. J Geophys Res. https://doi.org/10.1029/2002JD002448

Reed SC, Cleveland CC, Townsend AR (2011) Functional ecology of free-living nitrogen fixation: a contemporary perspective. Annu Rev Ecol Evol Syst 42:489–512

Richards LA (1931) Capillary conduction of liquids through porous mediums. J Appl Phys 1(5):318–333

Riley WJ, Matson PA (2000) NLOSS: a mechanistic model of denitrified N$_2$O and N$_2$ evolution from soil. Soil Sci 165(3):237–249

Riley WJ, Maggi F, Kleber M, Torn MS, Tang JY, Dwivedi D, Guerry N (2014) Long residence times of rapidly decomposable soil organic matter: application of a multi-phase, multi-component, and vertically resolved model (BAMS1) to soil carbon dynamics. Geosci Model Dev 7(4):1335–1355

Schimel JP (2018) Life in dry soils: effects of drought on soil microbial communities and processes. Annu Rev Ecol Evol Syst 49:409–432

Schimel J, Balser TC, Wallenstein M (2007) Microbial stress-response physiology and its implications for ecosystem function. Ecology 88(6):1386–1394

Schreiber F, Wunderlin P, Udert KM, Wells GF (2012) Nitric oxide and nitrous oxide turnover in natural and engineered microbial communities: biological pathways, chemical reactions, and novel technologies. Front Microbiol 3:372

Schwinning S, Sala OE (2004) Hierarchy of responses to resource pulses in arid and semi-arid ecosystems. Oecologia 141(2):211–220

Sexstone AJ, Parkin TB, Tiedje JM (1985) Temporal response of soil denitrification rates to rainfall and irrigation 1. Soil Sci Soc Am J 49(1):99–103

Six J, Conant RT, Paul EA, Paustian K (2002) Stabilization mechanisms of soil organic matter: implications for C-saturation of soils. Plant Soil 241(2):155–176

Skiba U, Smith KA (2000) The control of nitrous oxide emissions from agricultural and natural soils. Chemosphere 2(3–4):379–386

Stark JM, Firestone MK (1995) Mechanisms for soil moisture effects on activity of nitrifying bacteria. Appl Environ Microbiol 61(1):218–221

Stern H, Dahni RR (2013) The distribution of climate zones across Australia: identifying and explaining changes during the past century, in 25th Conference on Climate Variability and Change. American Meteorological Society, Austin

Tang JY, Riley WJ (2019) A theory of effective microbial substrate affinity parameters in variably saturated soils and an example application to aerobic soil heterotrophic respiration. J Geophys Res Biogeosci 124(4):918–940

Thomas RJ, Asakawa NM (1993) Decomposition of leaf litter from tropical forage grasses and legumes. Soil Biol Biochem 25(10):1351–1361

Tiedje JM, Sexstone AJ, Myrold DD, Robinson JA (1983) Denitrification: ecological niches, competition and survival. Antonie van Leeuwenhoek 48(6):569–583

Tietjen B, Schlaepfer DR, Bradford JB, Lauenroth WK, Hall SA, Duniway MC, Wilson SD et al (2017) Climate change-induced vegetation shifts lead to more ecological droughts despite projected rainfall increases in many global temperate drylands. Glob Chang Biol 23(7):2743–2754

Vargas R, Detto M, Baldocchi DD, Allen MF (2010) Multiscale analysis of temporal variability of soil CO$_2$ production as influenced by weather and vegetation. Glob Chang Biol 16(5):1589–1605

Wang W, Fang J (2009) Soil respiration and human effects on global grasslands. Glob Planet Chang 67(1–2):20–28

Warren CR (2014) Response of osmolytes in soil to drying and rewetting. Soil Biol Biochem 70:22–32

Wickland KP, Neff JC (2008) Decomposition of soil organic matter from boreal black spruce forest: environmental and chemical controls. Biogeochemistry 87(1):29–47

Wolery TJ (1992) EQ3/6: A software package for geochemical modeling of aqueous systems: package overview and installation guide (version 7.0). Lawrence Livermore National Laboratory Livermore, CA

Xiang SR, Doyle A, Holden PA, Schimel JP (2008) Drying and rewetting effects on C and N mineralization and microbial activity in surface and subsurface California grassland soils. Soil Biol Biochem 40(9):2281–2289

Xie P, Chen M, Shi W (2010) CPC unified gauge-based analysis of global daily precipitation. In Preprints, 24th conference on hydrology, Atlanta, GA, American Meteor Society, vol 2. https://www.esrl.noaa.gov/psd/

Xu Y, Xu Z, Cai Z, Reverchon F (2013) Review of denitrification in tropical and subtropical soils of terrestrial ecosystems. J Soils Sediments 13(4):699–710

Yan Z, Liu C, Todd-Brown KE, Liu Y, Bond-Lamberty B, Bailey VL (2016) Pore-scale investigation on the response of heterotrophic respiration to moisture conditions in heterogeneous soils. Biogeochemistry 131(1–2):121–134

Yan Z, Bond-Lamberty B, Todd-Brown KE, Bailey VL, Li S, Liu C, Liu C (2018) A moisture function of soil heterotrophic respiration that incorporates microscale processes. Nat Commun 9(1):2562

Yu K, Saha MV, D'Odorico P (2017) The effects of interannual rainfall variability on tree-grass composition along Kalahari rainfall gradient. Ecosystems 20(5):975–988

Zhang X, Wan H, Zwiers FW, Hegerl GC, Min SK (2013) Attributing intensification of precipitation extremes to human influence. Geophys Res Lett 40(19):5252–5257